Biophysical Chemistry 202 (2015) 32–39

Contents lists available at ScienceDirect

Biophysical Chemistry

journal homepage: http://www.elsevier.com/locate/biophyschem

Explicit analytic equations for multimolecular thermal melting curves

Albrecht Böttcher [a], Danny Kowerko [b,*], Roland K.O. Sigel [b]

[a] Chemnitz University of Technology, Department of Mathematics, 09107 Chemnitz, Germany
[b] University of Zurich, Department of Chemistry, Winterthurerstrasse 190, 8057 Zurich, Switzerland

HIGHLIGHTS

- Exact mathematical solutions to plot or analyze thermal melting curves are presented.
- The derivation of explicit equations for molecularities n = 1 to n = 4 is given.
- Explicit equations for molecularities n > 3 are new to the field.
- A software tool is provided to support fast plots and data export for any molecularity.
- The equations facilitate curve fit based analysis of thermal melting curves.

GRAPHICAL ABSTRACT

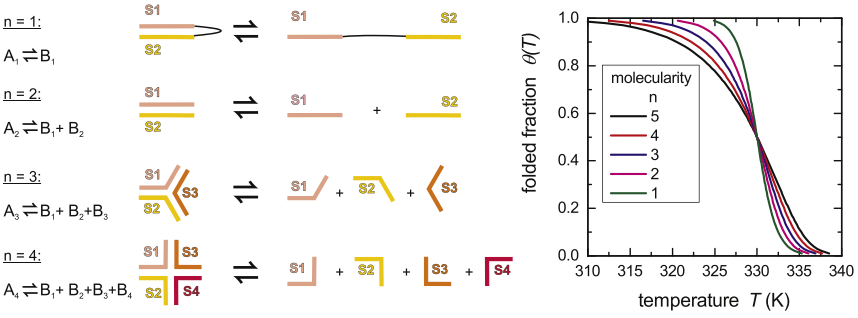

ARTICLE INFO

Article history:
Received 28 February 2015
Received in revised form 31 March 2015
Accepted 1 April 2015
Available online 9 April 2015

Keywords:
Thermal melting curve
Multimolecular reaction
Curve fitting
Van't Hoff analysis
Thermodynamic parameter
Software

ABSTRACT

The analysis of thermal melting curves requires the knowledge of equations for the temperature dependence of the relative fraction of folded and unfolded components. To implement these equations as standard tools for curve fitting, they should be as explicit as possible. From the van't Hoff formalism it is known that the equilibrium constant and hence the folded fraction is a function of the absolute temperature, the van't Hoff transition enthalpy, and the melting temperature. The work presented here is devoted to the mathematically self-contained derivation and the listing of explicit equations for the folded fraction as a function of the thermodynamic parameters in the case of arbitrary molecularities. Part of the results are known, others are new. It is in particular shown for the first time that the folded fraction is the composition of a universal function which depends solely on the molecularity and a dimensionless function which is governed by the concrete thermodynamic regime but is independent of the molecularity. The results will prove useful for extracting the thermodynamic parameters from experimental data on the basis of regression analysis. As supporting information, open-source Matlab scripts for the computer implementation of the equations are provided.

1. Introduction

The thermodynamic stability of conformations adopted by biomolecules (nucleic acids, proteins) is often quantified by thermal melting experiments [1]. Heating a sample with species *A* usually leads to their dissociation, unfolding, or denaturation into a state of species *B*. To discriminate the species *A* and *B* experimentally various physical observables (PO) can be monitored, including (UV) absorbance, circular dichroism (CD), fluorescence (e.g. Förster Resonance Energy Transfer), and nuclear magnetic resonance (NMR) signals [1,2]. Experimental thermal melting curves show one of these physical measures as a function of the absolute temperature *T* and give a visual proof for the transition from *A* to *B*. This approach has been successfully applied for decades [3–5] and has gained great popularity in the thermodynamic

* Corresponding author. Tel.: +41 44 635 6596.
E-mail addresses: aboettch@mathematik.tu-chemnitz.de (A. Böttcher), danny.kowerko@chem.uzh.ch (D. Kowerko), roland.sigel@chem.uzh.ch (R.K.O. Sigel).

http://dx.doi.org/10.1016/j.bpc.2015.04.001
0301-4622/

characterization of proteins and nucleic acids for intra- and intermolecular folding reactions [1,6].

Molecular multiplexes of molecularities larger than two exist for proteins [7,8] as well as for nucleic acids in large variety, e.g., DNA and RNA 3-, 4-, and 5-way junctions [9–13], triplex DNA/RNA [1,14], G-quadruplex DNA/RNA [14–18], i-motif DNA/RNA [18,19], or DNA-linked materials [20], and are an important part of current research. Their thermodynamic characterization on the basis of thermal melting experiments as in [2] is sparse. A shortcoming is that the mathematically exact description of thermal melting curves is not explicitly available throughout the whole scale of molecularities. Although theoretical derivations based on van't Hoff's formalism which describe melting transitions by two-state transition theory (that is, in the absence of intermediate states between A and B) exist for any molecularity n, see [21,22], explicit equations describing the entire experimental melting curve including the baselines are well known for $n \le 2$ only, see [22–25]. Such an equation is in [8] for $n = 3$, but to the best of our knowledge, explicit equations are missing for $n > 3$.

It is not the scope of this paper to face the question whether the two-state transition theory is applicable to the above mentioned multimers. Also beyond the scope of the paper are the derivation and discussion of the mathematical formalisms for other denaturation experiments, for example, for those in which external conditions are changed to unfold structures by means of chemicals like urea [26], pressure [27], or pH [28]. We will focus our attention on the derivation of implicit and explicit analytical equations for thermal melting transitions that have the potential to be of use for testing the two-state assumption or the type of multimer melting.

The mathematical description of an experimental thermal melting curve is usually given by the formula $PO(T) = BL_A \cdot \theta(T) + BL_B \cdot (1 - \theta(T))$ where BL_A and BL_B are the so-called baseline functions of A and B and θ is the relative fraction of A. Throughout this paper, we will be using the terms folded and unfolded for the annealed fraction θ and the melted fraction $1 - \theta$, as widely used for nucleic acids, respectively. But as our derivations are generally applicable, depending on the system, "folded" can also mean "bound, docked, structured, native, complexed, assembled, hybridized", and "unfolded" can be replaced with "unbound, undocked, unstructured, denatured, dissociated, or dehybridized". The mathematical description of the baselines as functions of the temperature is not within the focus of this article, and therefore we refer the reader to [1,2,22,24] for more information on this subject.

For n-molecular equilibria governed by the law $A_n \rightleftharpoons B_1 + \cdots + B_n$, general equations that link $\theta(T)$ and $K_c(T)$ are reviewed and summarized in [21,22]. A numerical solution to the problem of plotting $\theta(T)$ for $n > 2$ is given in [2]. Here we will present three different ways to obtain $\theta(T)$: (i) by elucidating exact graphical solutions for any molecularity, (ii) by presenting exact numerical solutions for any molecularity, and (iii) by deriving exact explicit equations for $1 \le n \le 4$ along with good approximations for $n \ge 5$. We are well aware of the fact that n-molecular two-state reactions with $n \ge 5$ are extremely unlikely, but we consider it as useful to embed the lower-molecular cases into the entire scale of all n because this reveals common features of all molecularities on the one hand and peculiarities of the cases $1 \le n \le 4$ on the other.

For each of the solutions (i), (ii), and (iii), open-source Matlab scripts are provided as supporting information along with a graphical user interface and an ascii-export option. By means of these tools, one can easily and instantly generate melting curves for arbitrary molecularities, which, in turn and with the due care concerning experimental data, can be used to perform model tests. Moreover, the Matlab scripts also produce plots of $\theta(T)$ and the first two derivatives $\theta'(T)$ and $\theta''(T)$.

The open-source codes for numerical solution (ii) as well as the explicit equations derived in (iii) can be used for regression analysis of experimental thermal melting curves describable by the aforementioned $PO(T)$ type equation with the purpose to extract thermodynamic parameters (ΔH, T_m, ΔS, and ΔG). We consider our equations as important ingredients to regression analysis, but we emphasize that these equations alone will not solve all problems. Deviations or distortions of thermal melting profiles can arise for numerous reasons, including aggregation, irreversibility, impurities, intermediates, non-2-state processes, and so forth. Thus, fitting to highly-parameterized models such as presented here should be attempted only when supported by other experimental approaches that validate the multi-molecular mechanism.

2. Mathematical background

2.1. The mathematical model

We consider a multimolecular equilibrium reaction assuming a two-state melting process of the form $A \rightleftharpoons B = m_1B_1 + \cdots + m_kB_k$. Fig. 1 exemplifies such reactions in the case of nucleic acids. As mentioned above, one typically monitors a PO (for example, an absorbance a) over a certain temperature range in order to determine the relative fraction $\theta_A = \theta_A(T)$ of molecules in state A as a function of the absolute temperature T. We abbreviate $\theta_A(T)$ to $\theta(T)$. Thus, $\theta_A(T) = \theta(T)$ and $\theta_B(T) = 1 - \theta(T)$.

It is assumed that $a(T)$ and $\theta(T)$ are related by an equation of the form

$$a(T) = (\alpha T + \beta)\theta(T) + (\gamma T + \delta)(1 - \theta(T)), \tag{1}$$

where $\alpha, \beta, \gamma, \delta$ are constants which describe the baselines BL_A and BL_B, that is, the affine linear behavior of $a(T)$ for $\theta(T)$ near 1 and 0. See [1,2,4,5,22] for background information. Under the assumption that the pressure is constant, van't Hoff's equation states that the equilibrium constant K_c satisfies the differential equation

$$\frac{d \ln K_c}{d(1/T)} = \frac{\Delta H}{R}, \tag{2}$$

where $R = 8.3145\,\mathrm{J/mol\,K}$ is the universal gas constant and $\Delta H (< 0)$ denotes the (temperature-independent) enthalpy change. The melting temperature T_m is defined by $\theta(T_m) = 1/2$. The equilibrium constant K_c is actually a function of θ, $K_c = f_n(\theta)$ with some function $f_n(\theta)$ determined by the molecularity $n = m_1 + \cdots + m_k$, and thus Eq. (2) is in fact a differential equation for $\theta = \theta(T)$.

2.2. Purpose of our study

We will show that $\theta(T)$ can be expressed in the form

$$\theta(T) = \varphi_n\left(\frac{\Delta H}{R}\left(\frac{1}{T} - \frac{1}{T_m}\right)\right) \tag{3}$$

or equivalently,

$$\theta(T) = \varphi_n(x) \quad \text{with} \quad x = \frac{\Delta H}{R}\left(\frac{1}{T} - \frac{1}{T_m}\right), \tag{4}$$

where $\varphi_n(x)$ is a function that depends solely on the molecularity n. Notice that both θ and x are dimensionless quantities. Thus, the functions $\varphi_n(x)$ describe universal laws, and all concrete chemical parameters are packed up together in the single quantity x via Eq. (4).

The purpose of this article is to give explicit formulas for $\varphi_n(x)$ if $n \le 4$ and to establish good approximations to $\varphi_n(x)$ for $n \ge 5$. The ability to compute $\theta = \varphi_n(x)$ is of major interest in the context of numerous biophysical experiments. For example, suppose we have the data $(T_j, a_j)_{j=1}^N$ of N measurements $a_j = a(T_j)$. Once the function $\varphi_n(x)$ is explicitly available, the right-hand side of Eq. (1) is completely specified

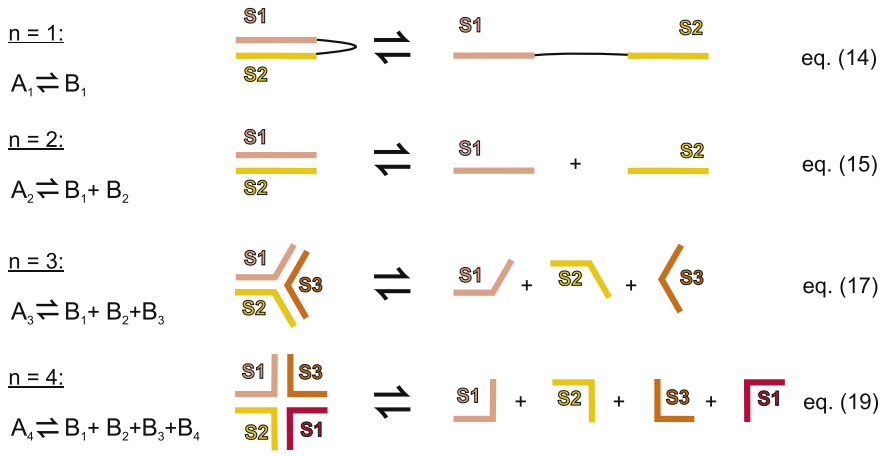

Fig. 1. Intra and intermolecular equilibria exemplified by a schematic representation of secondary structure elements as occurring in nucleic acids like hairpins, duplexes, 3- and 4-way junctions. Here, the structural elements B_k are single strands of oligonucleotides S_k. For thermal melting experiments, usually equal strand concentrations $[S_k]$ are used. The relative fraction of A_n, denoted by θ, can accordingly be given as a function of the temperature in an explicit form by the equations indicated on the right.

up to the six parameters α, β, γ, δ, ΔH, T_m. These six parameters may then be determined by solving the least squares problem

$$\sum_{j=1}^{N}\left(a\left(T_j\right)-a_j\right)^2\to min.$$

If α, β, γ, δ are determined by baseline approximation, we are left with even only the two parameters T_m and ΔH. However, we here like to reinforce our warning from the introduction: although the explicit functions $\varphi_n(x)$ solve the fitting problem theoretically, in practice one should act with the necessary diligence and strive for additional pieces of information.

For $n = 1$ and $n = 2$, explicit equations $\theta(T) = \theta(T, \Delta H, T_m)$ are known from the literature. In our notation, these equations may be written in the form of Eq. (3) or (4) with

$$\varphi_1(x)=\frac{1}{1+e^x},\quad \varphi_2(x)=1-\frac{e^x}{4}\left(\sqrt{1+8e^{-x}}-1\right). \tag{5}$$

The first of these equations is well known: see, e.g., formula (20–67) of [23] or formula (5) of [29]. The second equation is also known: see, e.g., Table 1 of [22], formula (13.26) of [24], formula (8) of [25], or formula (4) of [26]. Notice that we could write the equations also as

$$\varphi_1(x)=1-\frac{1}{1+e^{-x}},\quad \varphi_2(x)=1-\frac{2}{1+\sqrt{1+8e^{-x}}}. \tag{6}$$

This is obvious for the first equation. The second equation in Eq. (6) follows from the identity $\sqrt{1+8e^{-x}}-1=8e^{-x}/\left(1+\sqrt{1+8e^{-x}}\right)$. We will re-derive these two equations here. An explicit expression for $\varphi_3(x)$ was given in [8] by having recourse to Cardano's formula for cubic polynomials. This expression is equivalent to our formula (17) below. We here derive an explicit formula for $\varphi_4(x)$ using Ferrari's formula for quartic polynomials [30, p. 4]. Although the formulas of Cardano and Ferrari are of immense historical importance and have influenced a great deal of present-day mathematics, their applications to concrete problems in practice are sparse. We therefore consider it as very noteworthy that just these formulas give handy exact equations for the melting curves of trimolecular and tetramolecular dissociation and binding reactions.

2.3. Van't Hoff analysis

The equilibrium constant for the reaction $A \rightleftharpoons B = m_1B_1 + \cdots + m_kB_k$ is

$$K_c=\frac{[B_1]^{m_1}\cdots[B_k]^{m_k}}{[A]},$$

and as θ is the fraction of species A and $1-\theta$ the fraction of species B, we have $[A]=\theta[A]_0$ and $[B_j]=m_j(1-\theta)[A]_0$, where $[A]_0$ stands for the total concentration. This yields

$$K_c=\frac{\prod m_j^{m_j}(1-\theta)^n[A]_0^n}{\theta[A]_0}=\frac{c(1-\theta)^n}{\theta}, \tag{7}$$

where $n = m_1 + \cdots + m_k$ and c is the constant $c=[A]_0^{n-1}\prod m_j^{m_j}$; see, e.g., [5, p. 312]. We denote the function on the right-hand side of Eq. (7) by $f_n(\theta)$, thus getting the equation $K_c = f_n(\theta)$. Van't Hoff's Eq. (2) may then be written as

$$\frac{d\,ln f_n(\theta)}{d(1/T)}=\frac{\Delta H}{R}. \tag{8}$$

From Eq. (8) we infer that

$$ln\,f_n(\theta)=\int\frac{\Delta H}{R}d(1/T)=\frac{\Delta H}{RT}+C$$

with an integration constant C. As $\theta = 1/2$ for $T = T_m$, it follows that $ln\,f_n(1/2) = \Delta H/(RT_m) + C$, and hence

$$ln\,f_n(\theta)-ln\,f_n(1/2)=\frac{\Delta H}{R}\left(\frac{1}{T}-\frac{1}{T_m}\right)=:x. \tag{9}$$

Clearly, the function $\psi_n(\theta) := ln\,f_n(\theta) - ln\,f_n(1/2)$ is nothing but the inverse of the function $\theta = \varphi_n(x)$. Taking into account that

$$f_n(\theta)=\frac{c(1-\theta)^n}{\theta}, \tag{10}$$

we obtain from Eq. (9) that

$$x=\psi_n(\theta)=n\,ln(1-\theta)-ln\,\theta+(n-1)ln\,2. \tag{11}$$

At this point the inverse of the function $\varphi_n(x)$ we are looking for is at our disposal.

3. Results

3.1. Graphical solution

Eq. (11) allows us to plot $x = (\Delta H/R)(1/T - 1/T_m)$ as a function of θ, and reflection of the plot at the bisector $x = \theta$ of the first quadrant gives the plot of θ as a function of $x = (\Delta H/R)(1/T - 1/T_m)$. In other terms, to plot the n-molecular scaled melting curve $\theta = \varphi_n(x)$ in the (x, θ) plane, we may simply plot the curve $\{(\psi_n(\theta), \theta) : 0.03 < \theta < 0.97\}$. This curve allows us to find θ at a given x graphically. Fig. 2 shows the graphs of some functions $\theta = \varphi_n(x)$, while Fig. 5(A) gives examples of the dependence of $\theta = \theta(T)$ (vide infra).

3.2. Numerical solution

If $f(\theta) = f_n(\theta)$ is given by Eq. (10), then taking the exponential of Eq. (11) yields the equation

$$\frac{(1-\theta)^n}{\theta} = \frac{e^x}{2^{n-1}}. \tag{12}$$

As the left-hand side of Eq. (12) is strictly decreasing on (0, 1), this equation has a unique solution $\theta \in (0, 1)$ for each x. After writing $\theta = 1 - y$, Eq. (12) reads $y^n/(1 - y) = e^x/2^{n-1}$, that is,

$$y^n + \frac{e^x}{2^{n-1}}y - \frac{e^x}{2^{n-1}} = 0. \tag{13}$$

For $n = 4$, an equation equivalent to this equation is in [2,7]. Eq. (13) is an algebraic equation of the degree n in y, which can be easily solved with today's mathematical software. For example, the case $n = 4$ appeared in [2] and was solved there using Wolfram Mathematica. To give another example, if $n = 10$ and $x = 3$, then the solution y and thus $\theta = 1 - y$ can be computed via Matlab using the following commands.

```
n=10; x=3;
if n == 1; y=1/(1+exp(-x)); else
yr=roots([1 zeros(1,n-2) exp(x)./2.^(n-1) -exp(x)./
2.^(n-1)]);
for j=1:1:n;
if imag(yr(j)) == 0 & yr(j) > 0 & yr(j) < 1; y=yr(j); end;
end; end;
theta=1-y.
```

The result is $\theta = 0.3489205$.

3.3. Explicit melting equations

3.3.1. Monomolecular reactions

For $n = 1$, Eq. (13) is linear and we obtain $y = e^x/(1 + e^x)$. As $\theta = 1 - y$, we arrive at the well known formulas

$$\theta = \varphi_1(x) = \frac{1}{1+e^x} = 1 - \frac{1}{1+e^{-x}}, \tag{14}$$

which we already cited in Eqs. (5) and (6).

3.3.2. Bimolecular reactions

If $n = 2$, then Eq. (13) is a quadratic equation whose solution y between 0 and 1 is

$$y = -\frac{e^x}{4} + \frac{e^x}{4}\sqrt{1+8e^{-x}} = \frac{e^x}{4}\left(\sqrt{1+8e^{-x}} - 1\right),$$

which is the formula we encountered in subsection 2.2, and as shown there, this yields the second formula in Eqs. (5) and (6):

$$\theta = 1 - y = \varphi_2(x) = 1 - \frac{2}{1+\sqrt{1+8e^{-x}}}. \tag{15}$$

Equivalent expressions are

$$\varphi_2(x) = \frac{2}{1+\frac{1}{\sqrt{1+8e^{-x}}}} - 1 = \frac{1 - 1/\sqrt{1+8e^{-x}}}{1+1/\sqrt{1+8e^{-x}}} = \frac{\sqrt{1+8e^{-x}} - 1}{\sqrt{1+8e^{-x}} + 1}. \tag{16}$$

3.3.3. Trimolecular reactions

In that case, Eq. (13) is a cubic equation and Cardano's formula [30, p.4] eventually gives

$$\theta = \varphi_3(x) = 1 - \sqrt[3]{\sqrt{\frac{e^{2x}}{8^2} + \frac{e^{3x}}{12^3}} + \frac{e^x}{8}} + \sqrt[3]{\sqrt{\frac{e^{2x}}{8^2} + \frac{e^{3x}}{12^3}} - \frac{e^x}{8}}. \tag{17}$$

This formula is a restatement of formula (A5) of [8]. An equivalent expression is

$$\varphi_3(x) = 1 + \frac{e^{x/3}}{\sqrt[3]{8}}\left(\sqrt[3]{w-1} - \sqrt[3]{w+1}\right) \text{ with } w = \sqrt{1 + \frac{e^x}{27}}. \tag{18}$$

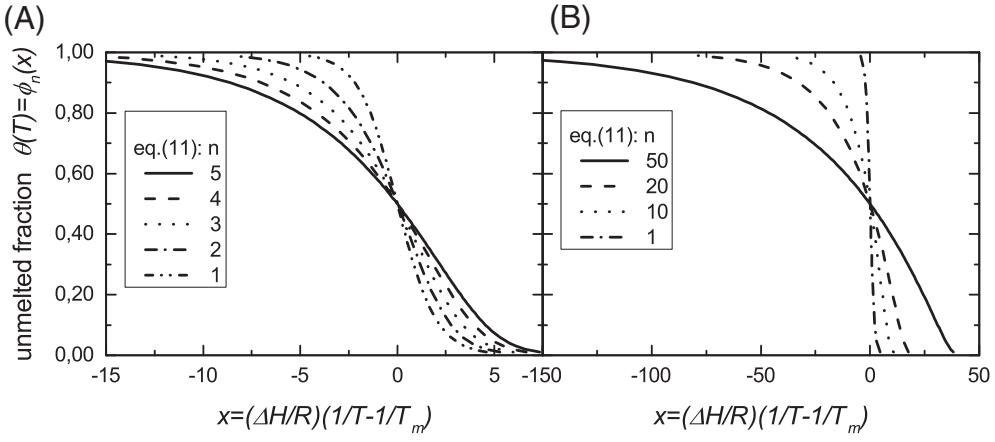

Fig. 2. Exact graphical representations of the curves $\theta = \varphi_n(x)$ for (A) low and (B) high molecularities n. Note that the steepness around $x = 0$, which corresponds to $T = T_m$, is decreasing with growing n. The graphs were obtained by plotting the curves according to Eq. (11).

3.3.4. Tetramolecular reactions

This time Eq. (13) has the degree 4 and we may have recourse to Ferrari's formula [30, p. 4]. Upon several computations and appropriate choices of signs one gets

$$\theta = \varphi_4(x) = 1 + \frac{1}{2}\sqrt{u-v} - \frac{1}{2}\sqrt{2\sqrt{u^2+uv+v^2} - (u-v)} \tag{19}$$

with

$$u = \sqrt[3]{\sqrt{\frac{e^{4x}}{128^2} + \frac{e^{3x}}{6^3}} + \frac{e^{2x}}{128}}, \quad v = \sqrt[3]{\sqrt{\frac{e^{4x}}{128^2} + \frac{e^{3x}}{6^3}} - \frac{e^{2x}}{128}}, \tag{20}$$

or equivalently,

$$u = \frac{e^{2x/3}}{4\sqrt[3]{2}}\sqrt[3]{r+1}, \quad v = \frac{e^{2x/3}}{4\sqrt[3]{2}}\sqrt[3]{r-1} \quad \text{with} \quad r = \sqrt{1 + \frac{2048}{27}e^{-x}}. \tag{21}$$

Fig. 3 shows that the functions (17) and (19), (20) indeed exactly match the melting curves obtained in Fig. 2 by a different construction.

3.3.5. Higher molecularities

For $n \geq 5$, formulas like those in the previous cases are no longer available. However, good approximations can be obtained from cut Taylor expansion combined with at most two Newton steps. Fig. 4 convincingly demonstrates the first-class quality of the approximations to the exact melting curves from Fig. 2.

The formula

$$\theta = \varphi_n(x) \approx \frac{1}{2} + \frac{n}{2(n-1)e^{x/n}}\left(n + e^{x/n} - \sqrt{n^2 + (2n-1)e^{2x/n} + 2e^{x/n}}\right) \tag{22}$$

is remarkably good for $x < 1$. The approximation

$$\theta = \varphi_n(x) \approx \frac{1}{2} - \frac{x}{2(n+1)} + \frac{1}{2}w(x) \tag{23}$$

with

$$w(x) = \frac{1 - \dfrac{x^2}{(n+1)^2}}{n+1-\dfrac{n-1}{n+1}x}\left(n\ln\left(1+\frac{x}{n+1}\right) - \ln\left(1-\frac{x}{n+1}\right) - x\right)$$

is fairly good for $x > 0$ as long as $\theta(x) > 0.1$. For $n = 5$ we may go with x almost until n. Finally, using

$$\theta = \varphi_n(x) \approx \frac{1}{n(n-1)}\left(n + \frac{e^x}{2^{n-1}} - \sqrt{\left(n + \frac{e^x}{2^{n-1}}\right)^2 - 2n(n-1)}\right) = \frac{2}{n + \dfrac{e^x}{2^{n-1}} + \sqrt{\left(n + \dfrac{e^x}{2^{n-1}}\right)^2 - 2n(n-1)}}. \tag{24}$$

we get good approximations for $x > n - 1/2$. Fig. 4 illustrates the approximations. The solid lines in these figures were obtained as in Fig. 2.

3.4. Derivatives

The derivatives of a function sometimes tell us more about the function than the function itself; see Fig. 5. We therefore want to mention the pleasant circumstance that in order to compute the derivatives of the functions $\varphi_n(x)$ we need not differentiate the explicit expressions we have given for these functions. It suffices to have recourse to Eq. (9). Moreover, the evaluation of the derivatives of $\varphi_n(x)$ can be reduced to evaluations of only $\varphi_n(x)$ itself. Indeed, Eq. (9) with $\theta = \varphi_n(x)$ reads $x = \ln f_n(\varphi_n(x)) - \ln f_n(1/2)$, and differentiating this equation we get $1 = (f_n'(\varphi_n(x))/f_n(\varphi_n(x))\varphi_n'(x)$, that is,

$$\varphi_n'(x) = \frac{f_n(\varphi_n(x))}{f_n'(\varphi_n(x))}. \tag{25}$$

Differentiating Eq. (25) again we obtain

$$\varphi_n''(x) = \left(1 - \frac{f_n(\varphi_n(x))f_n''(\varphi_n(x))}{f_n'(\varphi_n(x))^2}\right)\frac{f_n(\varphi_n(x))}{f_n'(\varphi_n(x))}.$$

Since $f_n(\theta) = c(1-\theta)^n/\theta$ is given by Eq. (10), this can be made more explicit to

$$\varphi_n'(x) = \frac{\varphi_n(x)(\varphi_n(x)-1)}{1 + (n-1)\varphi_n(x)} \tag{26}$$

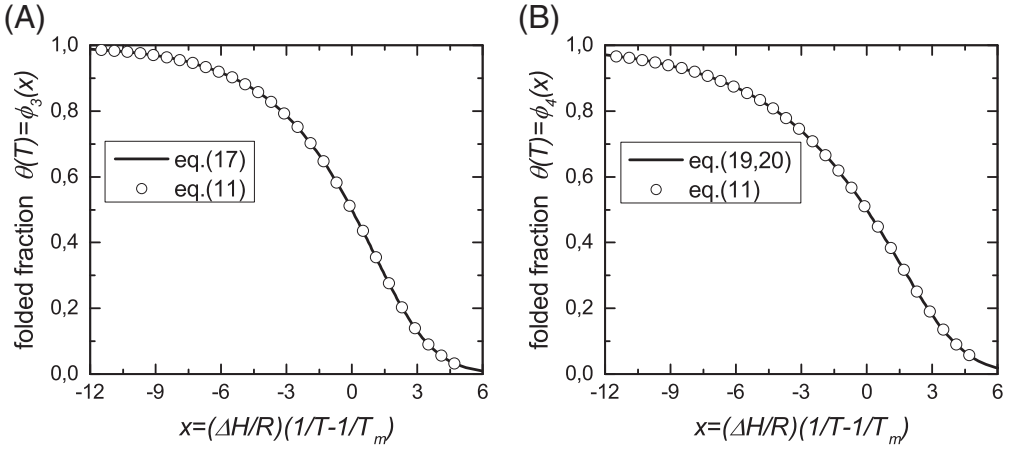

Fig. 3. Graphical validation of the explicit melting equations for $n = 3$ and $n = 4$. The graph of $\theta = \varphi_3(x)$ (solid line) and some values of function (17) (circles) in (A), and the graph of $\theta = \varphi_4(x)$ (solid line) and a few values of function (19) (circles) in (B). The solid lines were drawn as in Fig. 2, that is, we simply plotted the curves $\{(\psi_n(\theta), \theta) : 0.03 < \theta < 0.97\}$ for $n = 3$ and $n = 4$. The pictures convincingly illustrate that formulas (17) and (19) give the corresponding melting curve with absolute precision.

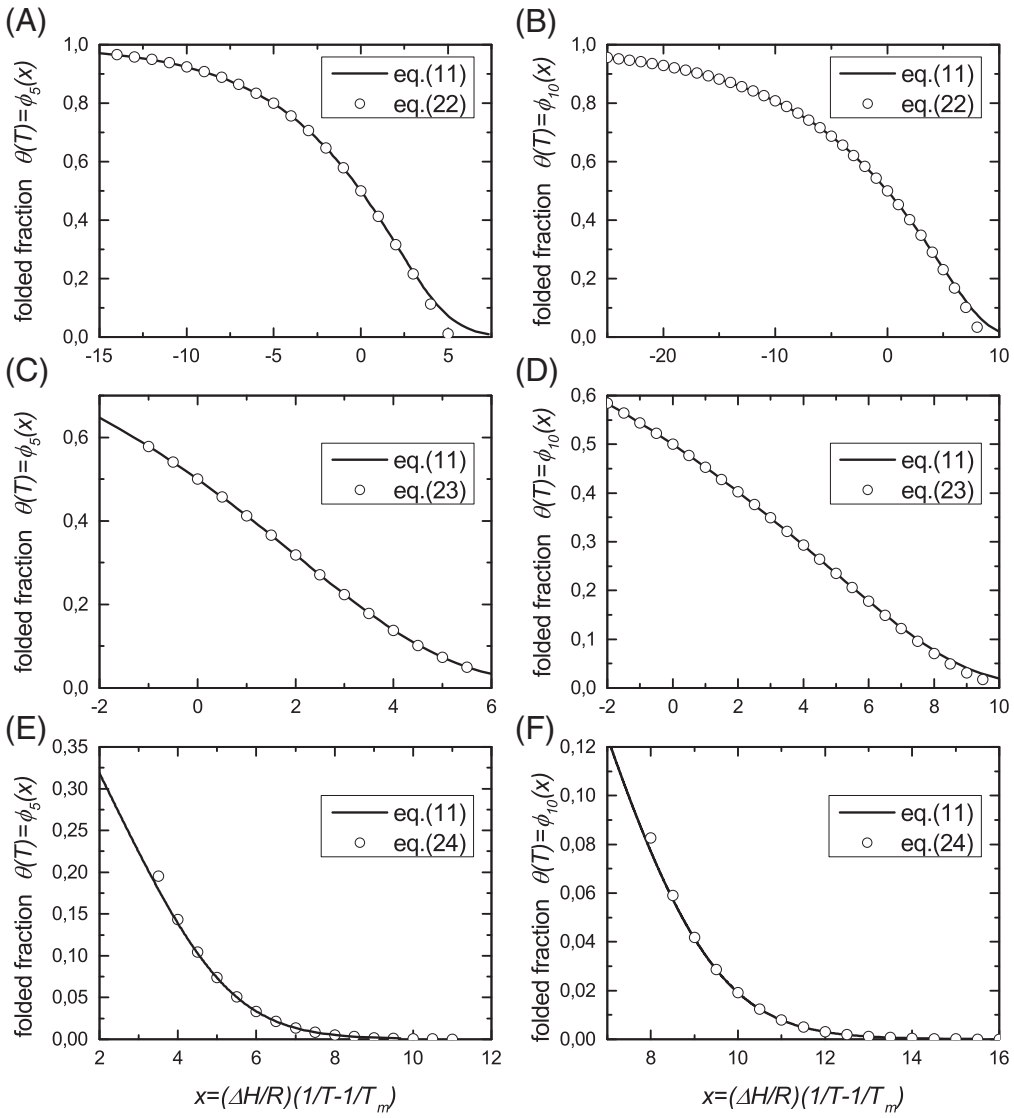

Fig. 4. Graphical validation of the approximations (22), (23), (24). The graphs of $\theta = \varphi_n(x)$ are drawn as solid lines in the left pictures for $n = 5$ and in the right pictures for $n = 10$. Some values of the functions (22), (23), (24) are plotted as circles in the upper, middle, and lower pictures, respectively.

and

$$\varphi_n''(x) = \frac{\varphi_n(x)(1-\varphi_n(x))\left(1-2\varphi_n(x)-(n-1)\varphi_n(x)^2\right)}{(1+(n-1)\varphi_n(x))^3}. \tag{27}$$

These formulas are consistent with those for $d\theta/d(1/T)$ and $d^2\theta/d(1/T)^2$ given in [22].

The shape broadening caused by increasing n and depicted in Fig. 5 is a well-known phenomenon in the DSC (Differential Scanning Calorimetry) community [25]. However, in several processes, ΔH also scales with increasing n, and hence the steepness in Fig. 5(A) is probably not a realistic reflection of what would happen in a real system and should therefore be treated with caution. In Fig. 5(B) and (D), potential melting transitions are shown for DNA 3-, 4-, and 5 way-junctions. The melting temperatures are adopted from Kadrmas et al. [13]. The respective thermodynamic parameters ΔH and ΔS were calculated using IDT SciTools as described elsewhere [31]. The basepair sequences of the single arms were concatenated in such a way that ΔH and ΔS match the experimentally found T_m values. For the 3-, 4-, and 5-way junction, this was roughly achieved with the thermodynamic data of almost 2 arms (12–13 BPs), 4 arms (28 BPs) and almost 4 of 5 arms (29 BPs), respectively. Such qualitative findings are in line with other studies of 3-way junctions [32,33] and 4-way junctions [34].

3.5. More general temperature dependence

We remark that our analysis is not restricted to constant right-hand sides in van't Hoff's equation. For example, it permits to take into account heat capacity changes, which are known to occur during heating/cooling cycles and to be modest for nucleic acids [1] but distinctive for proteins [35]. To see this, it is more to convenient to write Eq. (8) in the equivalent form $d\ ln\ f_n(\theta)/dT = -\Delta H/(RT^2)$. For a temperature dependent enthalpy change $\Delta H = \Delta H(T)$, the solution to this equation is

$$ln\ f_n(\theta) - ln\ f_n(1/2) = -\frac{1}{R}\int_{T_m}^{T} \frac{\Delta H(\tau)}{\tau^2} d\tau.$$

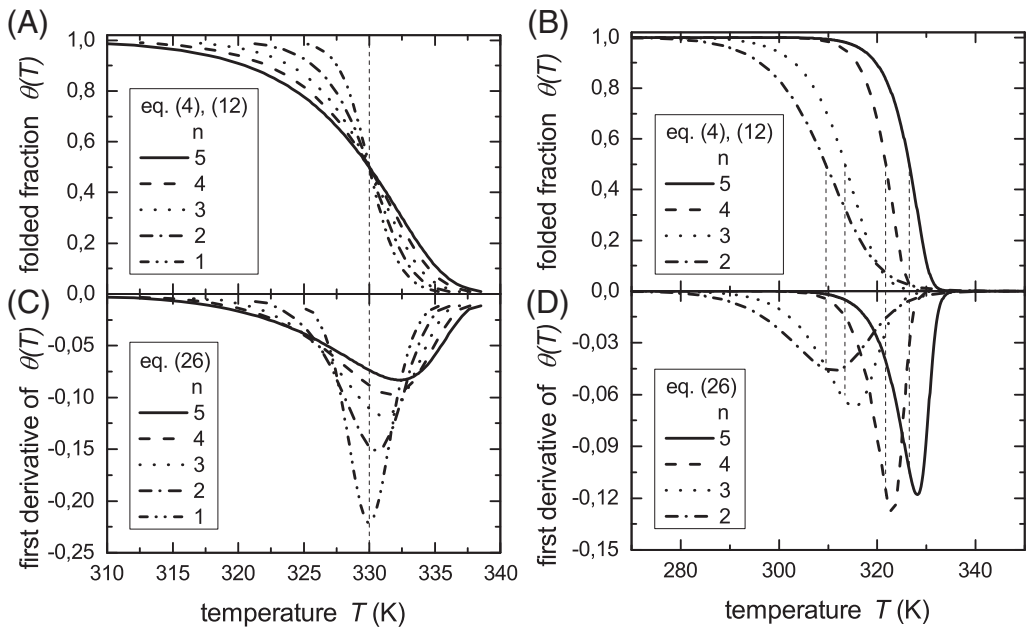

Fig. 5. The graphs of the functions $\theta = \theta(T)$ (A and B) and of the derivative $\theta'(T)$ (B and D) in the cases considered in Fig. 2(A) for $\Delta H/R = -100\ 000$ K and $T_m = 330$ K. The plots were obtained using Eqs (4), (12), (26). The plots in (A) reveal that the melting curves become flatter with increasing molecularity n. The plots in (C) convincingly show that, as already observed in [22], the minimum of the derivative $\theta'(T)$ moves to the right as the molecularity n increases. This phenomenon is hardly seen in (A). Plots (B) and (D) exemplify potential melting transitions of DNA 3-, 4-, and 5-way junctions (n = 3, 4, and 5, respectively). For details, see the text.

(Since T is the upper bound in the integral, we denoted the integration variable by τ.) This gives

$$\theta(T) = \varphi_n(x) \quad \text{with} \quad x = -\frac{1}{R}\int_{T_m}^{T} \frac{\Delta H(\tau)}{\tau^2} d\tau. \tag{28}$$

Clearly, this may also be written as

$$\theta(T) = \varphi_n(x) \ \text{ with } x = Q(T) - Q(T_m) \ \text{ and } \ Q(T) = -\frac{1}{R}\int_{T_0}^{T} \frac{\Delta H(\tau)}{\tau^2} d\tau, \tag{29}$$

where T_0 is any reference temperature. Two concrete situations are as follows.

(a) Suppose we have a nonzero heat capacity change $\Delta C_p = \partial \Delta H/\partial T$, which need not to be constant. Then

$$\Delta H(T) = \Delta H(T_m) + \int_{T_m}^{T} \Delta H(\sigma) d\sigma,$$

and inserting this in Eq. (28) we get

$$\begin{aligned} x &= -\frac{1}{R}\int_{T_m}^{T} \frac{\Delta H(T_m)}{\tau^2} d\tau - \frac{1}{R}\int_{T_m}^{T} \frac{1}{\tau^2}\int_{T_m}^{\tau} \Delta C_p(\sigma) d\sigma\, d\tau \\ &= \frac{\Delta H(T_m)}{R}\left(\frac{1}{T} - \frac{1}{T_m}\right) - \frac{1}{R}\int_{T_m}^{T} \Delta C_p(\sigma) \int_{\sigma}^{T} \frac{1}{\tau^2} d\tau\ d\sigma \\ &= \frac{\Delta H(T_m)}{R}\left(\frac{1}{T} - \frac{1}{T_m}\right) - \frac{1}{R}\int_{T_m}^{T} \Delta C_p(\sigma)\left(\frac{1}{\sigma} - \frac{1}{T}\right) d\sigma. \end{aligned} \tag{30}$$

Obviously, this could also be written as $Q(T) - Q(T_m)$ with

$$Q(T) = \frac{\Delta H(T_m)}{RT} - \frac{1}{R}\int_{T_m}^{T} \Delta C_p(\sigma)\left(\frac{1}{\sigma} - \frac{1}{T}\right) d\sigma.$$

In the special case where ΔC_p is constant, formula (30) can easily be simplified to

$$x = \frac{\Delta H(T_m)}{R}\left(\frac{1}{T} - \frac{1}{T_m}\right) - \frac{\Delta C_p}{R} ln\frac{T}{T_m} + \frac{\Delta C_p}{R}\left(1 - \frac{T_m}{T}\right), \tag{31}$$

that is, in this case we have Eq. (28) with x given by Eq. (31). Equivalently, we obtain formula (29) with $Q(T)$ defined by

$$Q(T) = \frac{\Delta H(T_m)}{RT} - \frac{\Delta C_p}{R}\left(ln\, T - \frac{T_m}{T}\right). \tag{32}$$

These formulas are well-known; see, e.g., [35,36].

(b) In [37], we encounter the equation $dlnf_n(\theta)/dT = -\Delta H/(RT^2)$ with $\Delta H = \Delta H(T)$ of the form

$$\Delta H(T) = \Delta H_0 + \frac{q_1}{T} + \frac{q_2}{T^2} + \frac{q_3}{T^3} + \cdots.$$

In that case the integral in Eq. (29) can easily be evaluated and we obtain

$$Q(T) = \frac{1}{RT}\left(\Delta H_0 + \frac{q_1}{2T^2} + \frac{q_2}{3T^3} + \frac{q_3}{4T^4} + \cdots\right) \tag{33}$$

for the type of temperature dependent enthalpy change at hand.

4. Conclusions

We have shown that the thermal melting curve $\theta = \theta(T)$ of an n-molecular two-state equilibrium reaction $A \rightleftharpoons B = m_1B_1 + \cdots + m_kB_k$ is of the form $\theta = \varphi_n(Q(T) - Q(T_m))$ with some function $Q(T)$ containing all chemical parameters and a universal function $\varphi_n(x)$ of a dimensionless variable x. If the right-hand side of the van't Hoff equation is

taken to be the constant $\Delta H/R$, then $Q(T) = \Delta H/(RT)$. The shape of the function $\varphi_n(x)$ depends exclusively on the sum $n = m_1 + \cdots + m_k$, we listed $\varphi_n(x)$ explicitly and in closed form for $n \leq 4$, and we indicated good approximations to $\varphi_n(x)$ for $n \geq 5$. We showed in particular that the famous but in practice rarely used formulas by Cardano and Ferrari for cubic and quartic equations provide us with closed-form expressions for the scaled melting function $\varphi_n(x)$ in the case of trimolecular and tetramolecular reactions. These will be of use in the regression analysis of experimental melting curves for reactions with triplexes, 3-way or 4-way junctions, or quadruplexes. Finally, the Supporting Information contains Matlab codes and a graphical user interface which compute $\varphi_n(x)$ and the derivatives $\varphi_n'(x)$, $\varphi_n''(x)$ and thus also $\theta(T)$, $\theta'(T)$, $\theta''(T)$ for arbitrary values of n.

Acknowledgments

We thank Sebastian König for proofreading the manuscript and for making a series of valuable remarks and suggestions. Sincere thanks go to Ben Schuler for helpful advice and for bringing several literature sources to our attention. We are greatly indebted to Mélodie Hadzic for her kind support with programming. We also want to mention that we derived essential benefit from Ilian Jelezarov's notes "Thermodynamics and Kinetics of Protein Folding" of a lecture course in Protein Biophysics held at the University of Zurich in 2013. Finally, we express our thanks to the referees for the exceptional care they devoted to the paper and for the many valuable hints and suggestions.

Financial support by the University of Zurich (P-73112-01-01 for Roland Sigel) (RKOS and Forschungskredit to DK (FK-13-108)) and the European Research Council (RKOS) ("MIRNA 259092") are gratefully acknowledged.

Appendix A. Supplementary data

Supplementary data to this article can be found online at http://dx.doi.org/10.1016/j.bpc.2015.04.001.

References

[1] J.-L. Mergny, L. Lacroix, Analysis of thermal melting curves, Oligonucleotides 13 (2003) 515–537.
[2] G. Vámosi, R.M. Clegg, Helix-coil transition of a four-way DNA junction observed by multiple fluorescence parameters, J. Phys. Chem. B 112 (2008) 13136–13148.
[3] J. Gralia, D.M. Crothers, Free energy of imperfect nucleic acid helices III: small internal loops resulting from mismatches, J. Mol. Biol. 78 (1973) 301–319.
[4] L.A. Marky, K.J. Breslauer, Calculating thermodynamic data for transitions of any molecularity from equilibrium melting curves, Biopolymers 26 (1987) 1601–1620.
[5] J.D. Puglisi, I. Tinoco Jr., Absorbance melting curves of RNA, Methods Enzymol. 180 (1989) 304–325.
[6] R. Owczarzy, B.G. Moreira, Y. You, M.A. Behlke, J.A. Walder, Predicting stability of DNA duplexes in solutions containing magnesium and monovalent cations, Biochemistry 47 (2008) 5336–5353.
[7] C.R. Johnson, P.E. Morin, C.H. Arrowsmith, E. Freire, Thermodynamic analysis of the structural stability of the tetrameric oligomerization domain of p53 tumor suppressor, Biochemistry 34 (1995) 5309–5316.
[8] J. Backmann, G. Schäfer, L. Wyns, H. Bönisch, Thermodynamics and kinetics of unfolding of the thermostable trimeric adenylate kinase from the archaeon sulfolobus acidocaldarius, J. Mol. Biol. 284 (1998) 817–833.
[9] Y. Liu, S.C. West, Timeline: happy hollidays: 40th anniversary of the holliday junction, Nat. Rev. Mol. Cell Biol. 5/11 (2004) 937–944.
[10] A. Oleksi, A.G. Blanco, R. Boer, I. Usón, J. AymamÃ-, A. Rodger, M.J. Hannon, M. Coll, Molecular recognition of a three-way DNA junction by a metallosupramolecular helicate, Angew. Chem. Int. Ed. 45 (2006) 1227–1231.
[11] S. Phongtongpasuk, S. Paulus, J. Schnabl, R.K.O. Sigel, B. Spingler, M.J. Hannon, E. Freisinger, Binding of a designed anti-cancer drug to the central cavity of an RNA three-way junction, Angew. Chem. Int. Ed. 52 (2013) 11513–11516.
[12] D. Shu, Y. Shu, F. Haque, S. Abdelmawla, P. Guo, Thermodynamically stable RNA three-way junction for constructing multifunctional nanoparticles for delivery of therapeutics, Nat. Nanotechnol. 6 (2011) 658–667.
[13] J.L. Kadrmas, A.J. Ravin, N.B. Leontis, Relative stabilities of DNA three-way, four-way and five-way junctions (multi-helix junction loops): unpaired nucleotides can be stabilizing or destabilizing, Nucleic Acids Res. 23 (1995) 2212–2222.
[14] R.A.J. Darby, M. Sollogoub, C. McKeen, L. Brown, A. Risitano, N. Brown, C. Barton, T. Brown, K.R. Fox, High throughput measurement of duplex, triplex and quadruplex melting curves using molecular beacons and a LightCycler, Nucleic Acids Res. 30 (9) (2002) e39.
[15] J.-L. Mergny, Kinetics of tetramolecular quadruplexes, Nucleic Acids Res. 33 (2005) 81–94.
[16] A.N. Lane, J.B. Chaires, R.D. Gray, J.C. Trent, Stability and kinetics of G-quadruplex structures, Nucleic Acids Res. 36 (2008) 5482–5515.
[17] J.B. Chaires, Human telomeric G-quadruplex: thermodynamic and kinetic studies of telomeric quadruplex stability: telomeric quadruplex stability, FEBS J. 277 (2010) 1098–1106.
[18] S.L.B. König, A.C. Evans, J.L. Huppert, Seven essential questions on G-quadruplexes, Biomol. Concepts 1 (2010) 197–213.
[19] H.A. Day, P. Pavlou, Z.A.E. Waller, i-Motif DNA: structure, stability and targeting with ligands, Bioorg. Med. Chem. 22 (2014) 4407–4418.
[20] O.-S. Lee, T.R. Prytkova, G.C. Schatz, Using DNA to link gold nanoparticles, polymers and molecules: a theoretical perspective, J. Phys. Chem. Lett. 1 (2010) 1781–1788.
[21] K.J. Breslauer, Extracting thermodynamic data from equilibrium melting curves for oligonucleotide order–disorder transitions, Methods Enzymol. 259 (1995) 221–242.
[22] R. Owczarzy, Melting temperatures of nucleic acids: discrepancies in analysis, Biophys. Chem. 117 (2005) 207–215.
[23] C.R. Cantor, Biophysical Chemistry: Part III: The Behavior of Biological Macromolecules, W.H. Freeman, San Francisco, 1980.
[24] R. Palais, C.T. Wittwer, Mathematical algorithms for high-resolution DNA melting analysis, Methods Enzymol. 454 (2009) 323–343.
[25] J.M. Sturtevant, Biochemical applications of differential scanning calorimetry, Annu. Rev. Phys. Chem. 38 (1987) 463–488.
[26] H. Backes, C. Berens, V. Helbl, S. Walter, F.X. Schmid, W. Hillen, Combinations of the *a*-helix-turn-*a*-helix motif of TetR with respective residues from LacI or 434Cro: DNA recognition, inducer binding, and urea-dependent denaturation, Biochemistry 36 (1997) 5311–5322.
[27] G. Hummer, S. Garde, A.E. Garcia, M.E. Paulaitis, L.R. Pratt, The pressure dependence of hydrophobic interactions is consistent with the observed pressure denaturation of proteins, Proc. Natl. Acad. Sci. U. S. A. 95 (1998) 1552–1555.
[28] F. Khan, A. Ahmad, M.I. Khan, Chemical, thermal and pH-induced equilibrium unfolding studies of Fusarium solani lectin, IUBMB life 59 (2007) 34–43.
[29] C.J. Wienken, P. Baaske, S. Duhr, D. Braun, Thermophoretic melting curves quantify the conformation and stability of RNA and DNA, Nucleic Acids Res. (2011) 1–10.
[30] P. Borwein, T. Erdélyi, Polynomials and Polynomial Inequalities, Springer, New York, 1995.
[31] R. Owczarzy, A.V. Tataurov, Y. Wu, J.a Manthey, K.a. McQuisten, H.G. Almabrazi, K.F. Pedersen, Y. Lin, J. Garretson, N.O. McEntaggart, C.A. Sailor, R.B. Dawson, A.S. Peek, IDT SciTools: a suite for analysis and design of nucleic acid oligomers, Nucleic Acids Res. 36 (Web Server issue) (2008) W163–W169.
[32] N.B. Leontis, W. Kwok, J.S. Newman, Stability and structure of three-way DNA junctions containing unpaired nucleotides, Nucleic Acids Res. 19 (1991) 759–766.
[33] J.E. Ladbury, J.M. Sturtevant, N.B. Leontis, The thermodynamics of formation of a three-strand, DNA three-way junction complex, Biochemistry 33 (1994) 6828–6833.
[34] D.H. Mathews, D.H. Turner, Experimentally derived nearest-neighbor parameters for the stability of RNA three- and four-way multibranch loops, Biochemistry 41 (2002) 869–880.
[35] W.J. Becktel, J.A. Schellman, Protein stability curves, Biopolymers 26 (1987) 1859–1877.
[36] J. Backmann, G. Schäfer, Thermodynamic analysis of hyperthermostable oligomeric proteins, Methods Enzymol. 334 (2001) 328–342.
[37] T. Galaon, V. David, Deviation from van't Hoff dependence in RP-LC induced by tautomeric interconversion observed for four compounds, J. Sep. Sci. 34 (2011) 1423–1428.